

Investigation of Structure in Liquid Hydrocarbons by X-ray Diffraction

BY J. W. OTVOS* AND H. MENDEL†

Koninklijke/Shell-Laboratorium, Amsterdam, Holland

(Shell Internationale Research Maatschappij N.V.)

(Received 9 October 1961)

The X-ray diffraction patterns of liquid mesitylene, cyclohexane, and benzene were obtained. For each one the calculated atomic and molecular scattering curves were subtracted and from the remainder an electron-density pair-distribution function was computed. The three functions were reasonable in shape and very similar to each other. A crude model, involving a spherically symmetric electron-density distribution around a central reference molecule, was found to account satisfactorily for the main features of all three experimental curves.

Introduction

The present paper is a continuation of our investigation of order phenomena in liquids by X-ray diffraction. In previous publications it has been shown (Mendel, 1962*a, b*) that by dispensing with 'sharpened intensities' and with the concept of point atoms, as introduced by Zernike & Prins (1927), it is possible to obtain reliable radial distribution curves free of spurious diffraction effects. The method has now been extended by removal of the intramolecular contributions to the distribution curve. This can be done when the structure of the molecules in the liquid is known. In this paper the method is applied to mesitylene, benzene, and cyclohexane. The result is an electron-density distribution function for the *intermolecular* vectors only. This function is different from that obtained by the Zernike & Prins method as extended by Debye (1925, 1927) and Menke (1932), which gives the probability of finding a certain distance between centers of molecules. The physical significance of our intermolecular distribution function will be evident from the derivation that follows.

It can be shown, by summing the scattered intensities due to all possible pairs of volume elements, that the total coherent scattering from a liquid sample of volume V relative to that from a classical electron, is

$$I_T(s) = \int_0^\infty \sigma_T(r) (\sin sr/sr) dr, \quad (1)$$

where $s = 4\pi \sin \theta/\lambda$ and $\sigma_T(r)$ is given by

$$\sigma_T(r) = 4\pi r^2 V \overline{\rho(o) \cdot \rho(r)}, \quad (2)$$

in which $\rho(o)$ represents the electron density at a point (o) and $\rho(r)$ that at a point a distance r away. The average over the whole sample of the product of densities a distance r apart is $\overline{\rho(o) \cdot \rho(r)}$. The factor $4\pi r^2 dr$ is proportional to the number of pairs a distance

r apart and is the weighting factor for the contribution of the distance r to the scattering. In the derivation of (1) it must be assumed that $\overline{\rho(o) \cdot \rho(r)}$ is independent of orientation.

Now since the total electron densities $\rho(o)$ and $\rho(r)$ are due to electrons from various atoms, 1, 2, 3, ... in the sample, we can separate the contributions of the atoms and write

$$\begin{aligned} \overline{\rho(o) \cdot \rho(r)} &= (\rho_1(o) + \rho_2(o) + \rho_3(o) + \dots) \\ &\quad \times (\rho_1(r) + \rho_2(r) + \rho_3(r) + \dots). \end{aligned} \quad (3)$$

There are three kinds of products to be distinguished here: those involving electrons

- (1) from the same atom,
- (2) from different atoms in the same molecule, and
- (3) from atoms in different molecules.

For these we will use the subscripts a for intra-atomic, m for intramolecular and i for intermolecular. Then

$$\overline{\rho(o) \cdot \rho(r)} = \overline{[\rho(o) \cdot \rho(r)]_a} + \overline{[\rho(o) \cdot \rho(r)]_m} + \overline{[\rho(o) \cdot \rho(r)]_i}. \quad (4)$$

The functions σ involving each of these are defined as in (2), and

$$\sigma_T(r) = \sigma_a(r) + \sigma_m(r) + \sigma_i(r). \quad (5)$$

By means of a Fourier transform of (1) one can also express $\sigma_T(r)$ in terms of the total scattered intensity:

$$\sigma_T(r)/r = 2/\pi \int_0^\infty s I_T(s) \sin sr ds. \quad (6)$$

In this form I_T includes the 'zero-angle' scattering, I_0 , which cannot be measured but whose Fourier transform can be shown to be

$$2/\pi \int_0^\infty s I_0(s) \sin sr ds = 4\pi r \bar{\rho}^2 V,$$

where $\bar{\rho}$ is the average electron density of the sample. Thus equation (6) now becomes

$$\sigma_T(r)/r = 2/\pi \int_{s_{\min}}^\infty s I_T^e(s) \sin sr ds + 4\pi r \bar{\rho}^2 V, \quad (7)$$

* Present address: Shell Development Co., Emeryville, California, U.S.A.

† Present address: Unilever Research Laboratory, Vlaarding, Holland.

where I_T^e is the experimentally determined coherent scattering on an absolute scale, very small angles being omitted.

We are now in a position to subtract the atomic and molecular parts of $\sigma_T(r)$ if the atomic scattering factors, f , are known, since the intensity scattered by free atoms can be expressed either as in (1) or in terms of f .

$$I_a(s) = \int_{s_{\min.}}^{\infty} \sigma_a(r) (\sin sr/sr) dr = \sum_i f_i^2(s). \quad (8)$$

Also, for a rigid molecule with interatomic distances, r_{ij} ,

$$I_m(s) = \int_{s_{\min.}}^{\infty} \sigma_m(r) (\sin sr/sr) dr = \sum_{i \neq j} f_i f_j \frac{\sin sr_{ij}}{sr_{ij}}. \quad (9)$$

Subtracting the Fourier transforms of (8) and (9) from (7) gives the intermolecular distribution function.

$$\sigma_i(r)/r = 2/\pi \int_{s_{\min.}}^{\infty} s I_L(s) \sin sr ds + 4\pi r \bar{\rho}^2 V, \quad (10)$$

where $I_L = I_T^e - I_a - I_m$. Division by $4\pi r V$ now gives directly the average density product, $[\rho(\sigma) \cdot \rho(r)]_i$, in which only the contributions from different molecules are counted. For brevity we will call this average product $P(r)$ in equation (11).

$$\begin{aligned} \sigma_i(r)/(4\pi r^2 V) &= P(r) \\ &= 1/(2\pi^2 r V) \int_{s_{\min.}}^{\infty} s I_L(s) \sin sr ds + \bar{\rho}^2. \quad (11) \end{aligned}$$

The methods for determining $I_L(s)$ so that (11) may be used to determine $P(r)$ are given in the following section.

Experimental technique and results

The diffraction pattern for mesitylene was obtained and those for benzene and cyclohexane were re-determined for comparison, using the experimental technique described previously (Van Panthaleon van Eck *et al.*, 1957, 1958). The sample is a liquid jet, usually 0.3 to 0.5 mm. in diameter, centered in a cylindrical camera and irradiated with monochromatized Cu $K\alpha$ radiation. Helium is circulated through the camera to eliminate parasitic air-scattering. For these hydrocarbon samples it was unnecessary to use any filters, to protect the film against fluorescent radiation, other than the 25μ aluminium foil which is always used to cut out visible light. Film densities were converted into intensities by an automatic microphotometer and then corrected for absorption and polarization.

The experimental intensity thus obtained, $I_{\text{exp.}}$, contains both incoherent and coherent scattering and

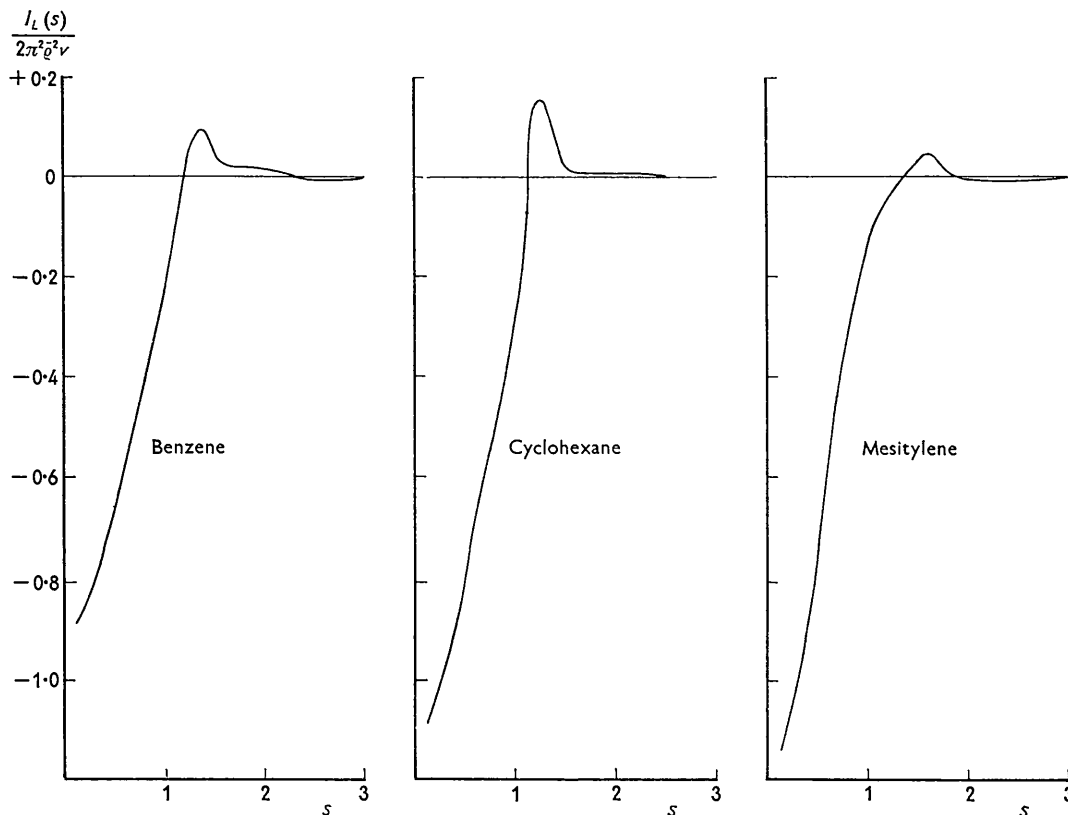


Fig. 1. The normalized function $I_L(s)$.

it must be multiplied by a scaling factor α , to convert it into an absolute intensity, as discussed by Krogh-Moe (1956) and Norman (1957).

$$\alpha I_{\text{exp.}} = I_T^e + I_{\text{inc.}}$$

The scaling factor may be expressed with the aid of equation (11), using the assumption that there is no overlap of non-bonded atoms. If this is true then $P(r)=0$ at $r=0$. Rewriting (11) with these conditions gives:

$$\int_0^\infty s^2 I_L(s) ds = -2\pi^2 V \bar{\rho}^2, \quad (13)$$

and substitution for I_L gives for α

$$\alpha = \frac{\int_0^\infty s^2 (I_{\text{inc.}}(s) + I_a(s)) ds + \int_0^\infty s^2 I_m(s) ds - 2\pi^2 V \bar{\rho}^2}{\int_0^\infty s^2 I_{\text{exp.}}(s) ds} \quad (14)$$

In practice it was found that I_L approached zero at rather small s values, around 3 or 4, and therefore it was unnecessary to carry out the integrations (summations) in (14) beyond that value. The value of α corresponding to the upper limit for which I_L has died out was used, and thus the function $P(r)$ was forced to start at the origin. The behaviour of $P(r)$ at small values of r could then be used as a criterion for the absence of systematic errors in the original data (Mendel, 1962a). Fig. 1 shows $I_L(s)$ for the three hydrocarbons and Fig. 2 gives the $P(r)$, the average intermolecular density product, normalized in each case to $\bar{\rho}^2=1$. It is evident that the functions are rather well-behaved near the origin and that they approach the limiting value, 1, rapidly above $r=5 \text{ \AA}$.

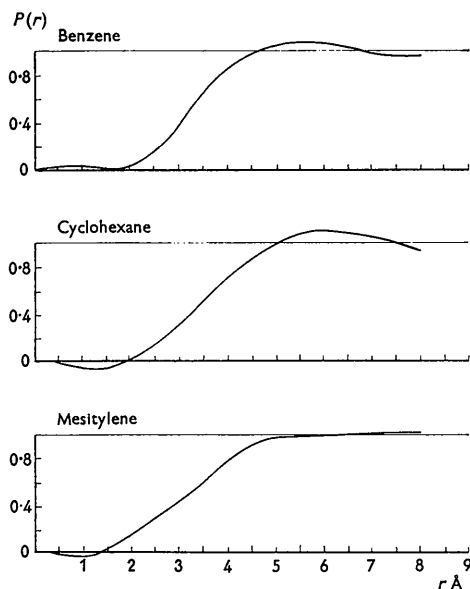


Fig. 2. Intermolecular electron-density product (experimental).

The most striking fact about Fig. 2 is the similarity of the curves to each other. They begin with a small initial slope, then rise nearly linearly in the central region and quickly approach the asymptote, with or without a broad maximum near the r value corresponding roughly to a molecular diameter. This similarity suggested that perhaps a rather simple model of the electron-density distribution in the liquid would suffice to account for the main features of the curves.

Explanation in terms of a model

We shall assume a spherically-symmetric electron-density distribution with the origin at the center of a spherical reference molecule. We will then calculate the average electron-density product over all possible pairs of volume elements a distance r apart, one of which is inside the reference molecule and the other outside. This average, $S(r)$, properly normalized, should correspond to $P(r)$ as defined by (11). The reference-molecule concept is justified because the electron distribution in the liquid looks the same on the average from each molecule. The spherical symmetry is, of course, arbitrary, but it is necessary for a convenient calculation.

Let the density within the central molecule be $\rho_x(x)$ and that outside, which is due to some average packing arrangement of similar molecules around the central one, be $\rho_y(y)$. (The distance from the origin is called x inside the central molecule and y outside. The unit of distance is the radius of the molecule.) Given a particular packing pattern, ρ_y is of course uniquely determined by ρ_x . However, the relationship between them is complex and it will suffice in this simple model to make a reasonable guess at ρ_y and to keep separate symbols for the two densities. In any case, ρ_y will be 0 at $y=1$ because the spheres surrounding the central one cannot penetrate and can at most be tangent to it.

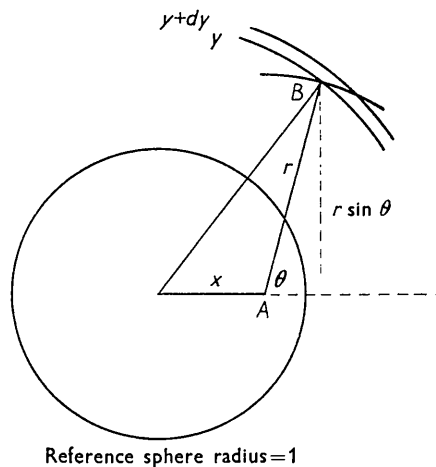


Fig. 3. Model of spherically symmetric electron distribution containing stick, AB , of length r .

Now to find $S(r)$ we put a rod of length r into the system in a random position with one end inside the reference sphere. The probability that the first end will be at A , a distance between x and $x+dx$ from the center, is $4\pi x^2 dx / (4\pi/3)$ (Fig. 3). The probability that at the same time the other end, B , is between y and $y+dy$ is given by the fraction of the spherical surface, $4\pi r^2$, with center at A that is enclosed between the spheres of radius y and $y+dy$. This enclosed surface is $2\pi r \sin \theta \cdot r d\theta$, and hence the probability is $\frac{1}{2} \sin \theta d\theta$. Furthermore we can see from Fig. 3 that the relation between θ and y is

$$\cos \theta = (y^2 - x^2 - r^2) / (2xr).$$

Elimination of θ gives $y dy / 2xr$ for the probability that the second end is between y and $y+dy$. The product of the two probabilities is the weighting factor for the occurrence of a density product, $\rho_x(x) \cdot \rho_y(y)$. Hence

$$S(r, x, y) = (3/2r) \cdot \rho_x(x) \rho_y(y) x dx y dy. \quad (15)$$

Now we must integrate over all possible values of x and y under the restriction that the distance between them is r . The upper limit of x is always 1 and the lower limit is either $(y-r)$ or $(r-y)$, depending on the length, r . But since $\rho_x(x)$ is symmetrical about the origin we can always use $(y-r)$. The upper limit of y is clearly $(r+1)$, while the lower limit is either 1 or $(r-1)$, depending on whether r is less than or greater than 2. The final expression for $s(r)$ then becomes

$$S(r) = (3/2r) \int_1^{r+1} y \rho_y(y) \int_{y-r}^1 x \rho_x(x) dx dy. \quad (16)$$

$$r < 2$$

$$r > 2r - 1.$$

Discussion

Three different functions, S , were calculated from (16) using the arbitrary function $1-x^2$ for $\rho_x(x)$. This has a rather flat maximum at the center, corresponding to the fact that there is no sharp concentration of charge at the center of a hydrocarbon molecule as there is, for example, in an atom. The three $\rho_y(y)$ functions tried are shown in Fig. 4 together with the resulting $S(r)$ curves normalized to $S(r)=1$ at the asymptote. Each $\rho_y(y)$ has a peak at $y=2$, the distance of closest approach, but the peaks have various heights to represent various degrees of uniformity of the packing pattern around the central molecule. Evidently the effect of increasing the peak height of $\rho_y(y)$ is to make the $S(r)$ curve steeper in the central portion and to produce a small hump near $y=2$.

The fit between the steepest $S(r)$ curve and the experimental $\rho(r)$ curve for benzene is reasonably good, as shown in Fig. 4(a). An even better fit could undoubtedly be made by sharpening the peak in $\rho_y(y)$. Mesitylene, on the other hand, fits best with the flattest $S(r)$ curve, as shown in Fig. 4(c), probably

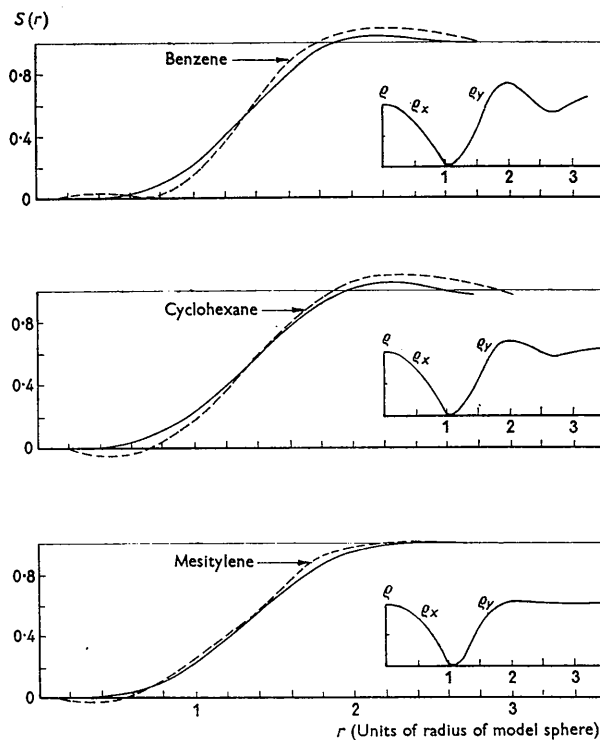


Fig. 4. Intermolecular electron-density product (calculated).

because it is much less spherical than benzene. The $\rho_y(y)$ in this case has almost no maximum and represents a smearing-out of the preferential distance of closest approach. Cyclohexane gives an intermediate slope and can be matched by the second curve, Fig. 4(b).

The functions $S(r)$ are not very sensitive to small variations in the $\rho_y(y)$ function, as can be seen from the range of examples given. The very fact that they can be made to agree so well with the experimentally measured intermolecular part of the electron density distribution function shows that there is no more detailed information available from X-ray diffraction alone on these liquid hydrocarbons. The situation is quite different, however, when heavy atoms are used, either by themselves, as in studies of liquid metals, or as substituents in hydrocarbons (Mendel, 1962b). Both $\rho_y(y)$ and $\rho_x(x)$ would then be considerably sharpened, with the result that $S(r)$ and $\rho(r)$ would give more information.

The authors are indebted to Mrs J. P. M. A. van Asselt-Ekkers for making the digital computer program and for help in the experimental work, and to Mr J. H. Kruizinga and Dr P. W. Kasteleyn for helpful discussions and for adaptation of the analog computer to the evaluation of the theoretical distribution curves.

References

- DEBYE, P. (1925). *J. Math. Phys.* **4**, 153.

DEBYE, P. (1927). *Phys. Z.* **28**, 135.
 KROGH-MOE, J. (1956). *Acta Cryst.* **9**, 951.
 MENKE, H. (1932). *Phys. Z.* **33**, 593.
 MENDEL, H. (1962a). *Acta Cryst.* **15**, 113.
 MENDEL, H. (1962b). *Acta Cryst.* **15**, 9.
 NORMAN, N. (1957). *Acta Cryst.* **10**, 370.

VAN PANTHALEON VAN ECK, C. L., MENDEL, H. & BOOG, W. (1957). *Disc. Faraday Soc.* **24**, 200.
 VAN PANTHALEON VAN ECK, C. L., MENDEL, H. & FAHRENFORT, J. (1958). *Proc. Roy. Soc. (London)*, **A**, **247**, 472.
 ZERNIKE, F. & PRINS, J. A. (1927). *Phys. Z.* **41**, 184.

Acta Cryst. (1962). **15**, 661

The Crystal Structure of Tetrachloro-*p*-Benzoquinone (Chloranil)

BY SHIRLEY S. C. CHU, G. A. JEFFREY, AND (IN PART) T. SAKURAI

The Crystallography Laboratory, The University of Pittsburgh, Pittsburgh 13, Pa., U.S.A.

(Received 24 January 1961 and in revised form 26 September 1961)

A three-dimensional structure analysis of chloranil, $C_6Cl_4O_2$, has been carried out to determine the positional parameters and the thermal motion of the molecules. A contemporary two-dimensional analysis has been reported by Ueda (1961) and the results are compared. The molecule has a quinoid structure and the quinoid ring is planar, with the oxygen and chlorine atoms displaced slightly (0.05 Å) out of the plane. The bond lengths and valence angles are normal, agreeing well with the data from 1245 tetrachlorobenzene and *p*-benzoquinone. The one unusual feature of the structure is a carbon to oxygen intermolecular separation of 2.85 Å, an observation which may be relevant to the well-known facility of chloranil to form charge transfer complexes. Because of this anomalous distance, a confirmation of the solution to the phase problem was obtained by an independent physical method. The orientation of the C-Cl bonds with respect to each other and the symmetry axis and, less precisely, the direction of the normal to the quinoid ring were measured by nuclear quadrupole resonance methods. These results completely confirmed the X-ray analysis.

Chloranil is compared with *p*-benzoquinone with respect to its molecular packing, anomalous dipole moment and infra-red spectrum.

Introduction

This work is a continuation of a study of the structure of halogen substituted benzene derivatives by combined X-ray analysis and nuclear quadrupole resonance spectroscopy. In an earlier paper on 1245 tetrachlorobenzene by Dean, Pollak, Craven & Jeffrey (1958), the primary emphasis had been on the n.q.r. technique as a means of measuring the directions of C-Cl bonds, and thereby providing evidence pertaining to the problem of over-crowded molecules, e.g. Harnik *et al.* (1954), Coulson & Stocker (1959), by a technique independent of diffraction studies. The X-ray work was secondary in that it served to establish that, within the accuracy of the X-ray analysis, there was complete agreement between the molecular information deduced from the two techniques. Further research, employing the n.q.r. method has been reported on the planarity of 1234 tetrachlorobenzene, by Dean, Richardson & Sakurai (1961), and on the structure of tetrachloro-hydroquinone by Sakurai (1961).

In this work, the primary emphasis has been on the X-ray analysis of the crystal structure and the role of the n.q.r. technique has been to check the validity of the solution of the phase problem.

Experimental

The C.P. grade chloranil, purchased from Matheson, Coleman and Bell Company (East Rutherford, New

Jersey), was purified by repeated recrystallization from benzene solution. The melting point of the purified material in a sealed tube is 291–293 °C. The crystals were grown from benzene solution by evaporation as thick, transparent, yellow plates elongated along *b*-axis. Twining occurred frequently on the (001) face.

The density of the crystal was determined by the floating method using a mixture of carbon tetrachloride and methyl iodide. An average density of 1.953 ± 0.005 g.cm.⁻³ was obtained from several measurements.

The unit-cell dimensions were measured from Weissenberg photographs about the principal axes, using both the Straumanis technique and an independent calibration with NaCl powder lines. The intensities were eye-estimated from multiple film equi-inclination Weissenberg photographs. The zero to fourth layers about the [*a*] and [*b*] and zero to seventh layers about the [*c*] were recorded. Of the 838 independent reflections within the Cu $K\alpha$ sphere, 620 were observed. The range of intensities measured was approximately 1700 to 1. No absorption corrections were applied. Crystals of approximately uniform cross-section with dimensions 0.10–0.12 mm. were used. The linear absorption coefficient for Cu $K\alpha$ radiation is 122.7 cm.⁻¹, and the effect of ignoring absorption corrections was estimated to give rise to errors of the order of 7% in structure amplitudes.